

Diffuse Neutron Scattering Study of Relaxor Ferroelectric $(1-x)\text{Pb}(\text{Zn}_{1/3}\text{Nb}_{2/3})\text{O}_3-x\text{PbTiO}_3$ (PZN- x PT)

D. La-Orauttapong*, J. Toulouse*, Z.-G. Ye[†], R. Erwin**, J.L. Robertson[‡] and W. Chen[†]

*Department of Physics, Lehigh University, Bethlehem, Pennsylvania 18015-3182

[†]Department of Chemistry, Simon Fraser University, Burnaby, British Columbia, Canada V5A 1S6

**NIST Center for Neutron Research, NIST, Gaithersburg, Maryland 20899-8562

[‡]Oak Ridge National Laboratory, Solid State Division, Oak Ridge, Tennessee 37831-6393

Abstract. Diffuse neutron scattering is a valuable tool to obtain information about the size and orientation of the polar nanoregions that are a characteristic feature of relaxor ferroelectrics. In this paper, we present new diffuse scattering results obtained on $\text{Pb}(\text{Zn}_{1/3}\text{Nb}_{2/3})\text{O}_3$ (PZN for short) and $(1-x)\text{Pb}(\text{Zn}_{1/3}\text{Nb}_{2/3})\text{O}_3-x\text{PbTiO}_3$ (PZN- x PT) single crystals (with $x=4.5$ and 9%), around various Bragg reflections and along three symmetry directions in the [100]-[011] zone. Diffuse scattering is observed around reflections with mixed indices, (100), (011) and (300), and along transverse and diagonal directions only. No diffuse scattering is found in longitudinal scans. The diffuse scattering peaks can be fitted well with a Lorentzian function, from which a correlation length is extracted. The correlation length increases with decreasing temperatures down to the transition at T_c , first following a Curie-Weiss law, then departing from it and becoming flat at very low temperatures. These results are interpreted in terms of three temperature regions: 1) dynamic polarization fluctuations (i.e. with a finite lifetime) at high temperatures, 2) static polarization reorientations (condensation of polar nanoregions) that can still reorient as a unit (relaxor behavior) at intermediate temperatures and 3) orientational freezing of the polar nanoregions with random strain fields in pure PZN or a structural phase transition in PZN- x PT at low temperatures. The addition of PT leads to a broadening of the diffuse scattering along the diagonal ([111]) relative to the transverse ([100]) direction, indicating a change in the orientation of the polar regions. Also, with the addition of PT, the polar nanoregions condense at a higher temperature above T_c .

INTRODUCTION

The single-crystal solid solution of the relaxor $\text{Pb}(\text{Zn}_{1/3}\text{Nb}_{2/3})\text{O}_3$ and ferroelectric PbTiO_3 , known as PZN- x PT is being considered as a promising candidate for the next generation material for electromechanical transducers [1]. This material has cubic perovskite structure at high temperatures but becomes slightly distorted at lower temperatures, where a transition to ferroelectric/relaxor phase takes place. Close to pure PZN (for PT contents below 9%), the low temperature phase is rhombohedral (R3m) and the material is a relaxor. For higher PT contents, the low temperature phase of the material becomes tetragonal (P4mm) and the relaxor character gradually vanishes. The boundary between the rhombohedral and tetragonal phases is called the “morphotropic phase boundary” (MPB), near which the crystals show remarkably large piezoelectric coef-

ficients [1, 2]. In earlier studies of a rhombohedral PZN-8%PT crystal in [001] bias electric fields, Park and Shrout [1] proposed that the origin of the large strain values observed is a rhombohedral-to-tetragonal phase transition. Later, Liu *et al.*[3] reported a similar behavior in PZN-4.5%PT. Very recently, Noheda *et al.*[4] have also observed a field-induced long-range tetragonal phase in both PZN-4.5%PT and PZN-8%PT using X-ray investigation, which is in agreement with the model proposed by Park and Shrout. Recently, the MPB has been characterized on single crystal samples by high resolution x-ray measurements [5, 6]. An orthorhombic phase (space group Pm) has been found in a narrow concentration range ($8\% < x < 11\%$) with near vertical phase boundaries between the tetragonal and rhombohedral phases. It can be described as a “matching” phase between the rhombohedral and tetragonal phase, which allows for a very easy reorientation of the polarization vector [7]. Recently, a model has been proposed that relates the structural features of the lead relaxor systems to their unusual polarization properties [8].

In addition to the above structural features, there exists another aspect of the polarization properties of relaxor systems, whose precise connection to these structural features has not been established yet. It is now a well recognized fact that, as relaxors are cooled from high temperature, the structural changes are preceded by appearance and growth of polar nanoregions. The first indirect observation of such regions came from birefringence measurements by Burns and Dacol on PMN and PZN [9]. These measurements revealed deviations of the birefringence $\Delta n(T)$ ($= n_{\parallel} - n_{\perp}$) from a linear temperature dependence, at temperature T_d , far above the temperature range in which PZN displays the relaxor behavior. These deviations were interpreted as marking the appearance of the polar regions. Since then, several other experimental observations have been reported that support the appearance of the polar regions in lead relaxors below 650 K for PMN and below 750 K for PZN. The most direct ones have come from measurements of diffuse X-ray or neutron scattering [10, 11]. Recently, we have reported diffuse neutron scattering results on a PZN single crystal that clearly indicate the development of short range order (a few unit cells) below approximately $T_d = 750\text{K}$ [12]. From the width of the diffuse scattering peak measured around the (011) Bragg reflection, we have been able to determine a correlation length or the size of the regions as a function of temperature (550 K-295 K). At the beginning of this range the temperature dependence of the correlation length is consistent with the Curie-Weiss dependence of the dielectric constant, which indicates the dynamic character of polarization. In this temperature range, therefore, the crystal behaves as a perfect paraelectric. At about $T^* = T_c + \delta T$ ($\delta T=40$ K), the deviation from the described above linear dependence indicates that the orientation of the polar regions becomes progressively more and more static. This progressive freezing is accompanied by the development of permanent strain fields that cause the Bragg intensity to increase rapidly (relief of extinction). In the present paper, we report the results of a diffuse neutron scattering study of several PZN- x PT single crystals with $x=0, 4.5,$ and 9% , using neutron scattering measurements. The goal of this study is 1) to extend the previous PZN study to other reciprocal lattice points, 2) to identify the onset of the local polar order more definitely and verify its temperature evolution and 3) to investigate the local structural and polar order at higher PT (x) concentrations.

EXPERIMENT

Single crystals of PZN and PZN-9%PT were grown by spontaneous nucleation from high temperature solutions, using an optimized flux composition of PbO and B₂O₃ [13]. The PZN-4.5%PT single crystal was grown by the top-cooling solution growth technique, using PbO flux [14]. All as-grown crystals used in the experiment exhibited a light yellow color and high optical quality.

The neutron experiments were carried out on the HB1 and HB1A triple-axis spectrometers at the High Flux Isotope Reactor (HFIR) of Oak Ridge National Laboratory and on the BT7 and BT9 triple-axis spectrometers at the NIST Center for Neutron Research (NCNR). The neutron energies used for the data displayed in this paper were 14.7 meV (2.36 Å) or 13.6 meV (2.45 Å) at HFIR and 14.7 meV (2.36 Å), 13.4 meV (2.47 Å) or 30.4 meV (1.64 Å) at NIST. Highly oriented pyrolytic graphite (002) (HOPG) was used to monochromate and analyze the incident and scattered neutron beams. An HOPG filter was used to suppress harmonic contamination. The samples were mounted on an aluminum sample holder, wrapped with copper foil and held in place with either an aluminum or a copper wire. To prevent contamination of the spectra by the scattering from aluminum, the sample holder was painted with gadolinium oxide or boron nitride paste, then loaded into a vacuum furnace. The measurements were made in the [100]-[011] scattering plane, which allowed access to the [100], [011], and [111] symmetry directions. Data were collected upon cooling from 650 K to 295 K around several reciprocal lattice points. No external electric field was applied.

RESULTS AND DISCUSSION

The diffuse scattering measurements have been made in the [100]-[011] zone, around many different reciprocal lattice points and in several directions. The diffuse scattering is found only for points with mixed (*hkl*) indices. In particular we have observed the diffuse scattering from (100), (011), and (300), which is consistent with the calculated diffuse scattering intensity on PMN reported by Mathan *et al.*[10] The diffuse scattering is observed along transverse and diagonal directions only. No diffuse scattering is found in a longitudinal direction. Like in many previous studies [15, 16], no diffuse scattering is observed at (200) reflection. This absence is either due to the soft mode, for which the structure factor is largest at the (200) in perovskites, or it must be related to the local order that develops below 600-700 K. Recent neutron diffuse scattering and the calculation model on PMN reported by Hirota *et al.*[17] have also confirmed the weak (200) diffuse scattering using a new concept of the phase-shifted condensed soft mode. A typical scan is presented in Fig. 1, which shows diffuse scattering around the (011) point for PZN, PZN-4.5%PT, and PZN-9%PT single crystals at different temperatures. With decreasing temperatures, the diffuse scattering peaks become broader, more extended in the [100] direction in pure PZN and in the [111] direction in PT-doped PZN. It also becomes broader with increasing PT concentration. Below the transition, the width of the diffuse scattering peaks remains constant, despite the fact that the Bragg peaks increase continuously. The diffuse scattering peaks are slightly asymmetric, which could be

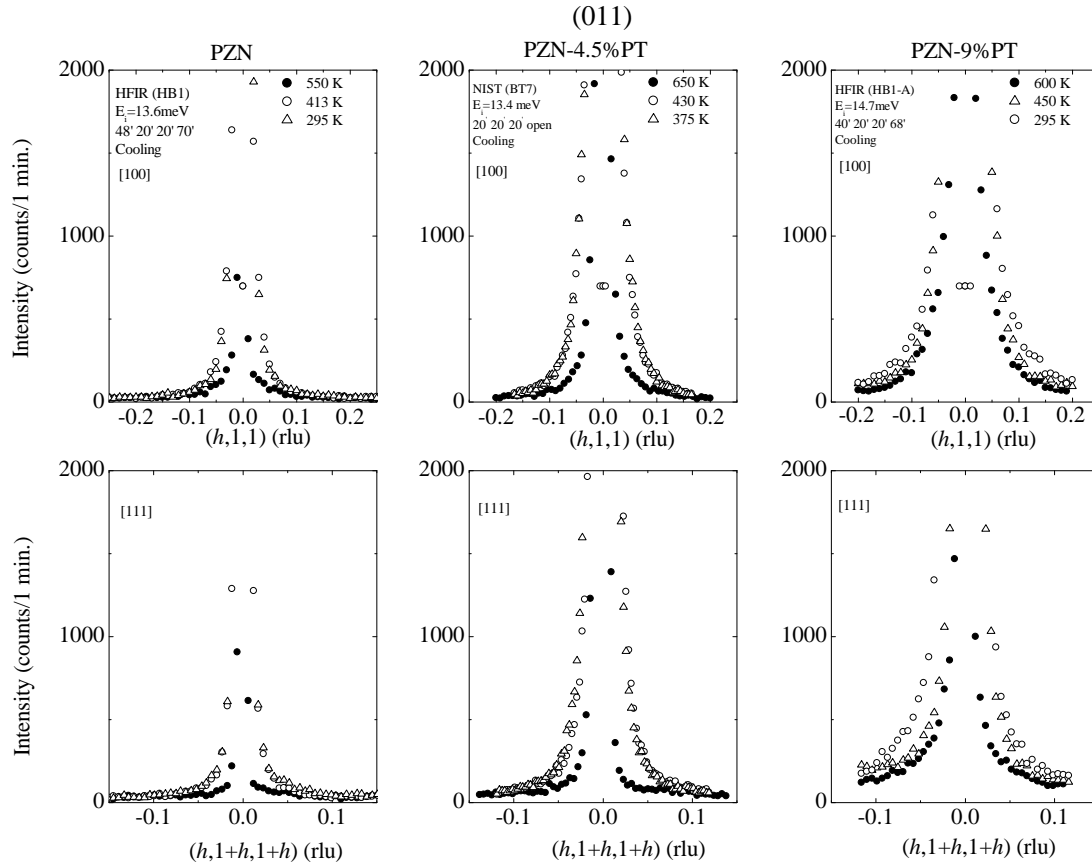


FIGURE 1. Neutron elastic scattering profile for PZN, PZN-4.5%PT, and PZN-9%PT at (011) point along [100] and [111] directions at different temperatures, showing the narrow Bragg peak and the broad diffuse scattering peak

related to a rather large deformation of the crystal lattice giving rise to Huang Scattering [18].

The temperature dependence of Bragg intensity presented in Fig. 2 reveals the phase transition temperature T_c . It is seen that pure PZN and PZN- x PT behave differently, the former undergoing a continuous structural transition while the latter undergoes abrupt structural changes. The rapid increase in Bragg intensity, observed for PZN below the transition $T_c \sim 413$ K, is due to the relief of extinction caused by a rapid increase in mosaicity [12]. In PZN-4.5%PT, the Bragg intensity increases moderately as the first transition is approached but abruptly drops at $T_c \sim 430$ K, when the crystal structure transforms from cubic to rhombohedral symmetry. In the 9%PT crystal, the first transition at 450 K is marked by a cusp while the second one at 340 K is marked by a discontinuous increase. From these results, it is evident that the addition of PT triggers sharp structural changes. This suggests that PT-doping enhances the local strain

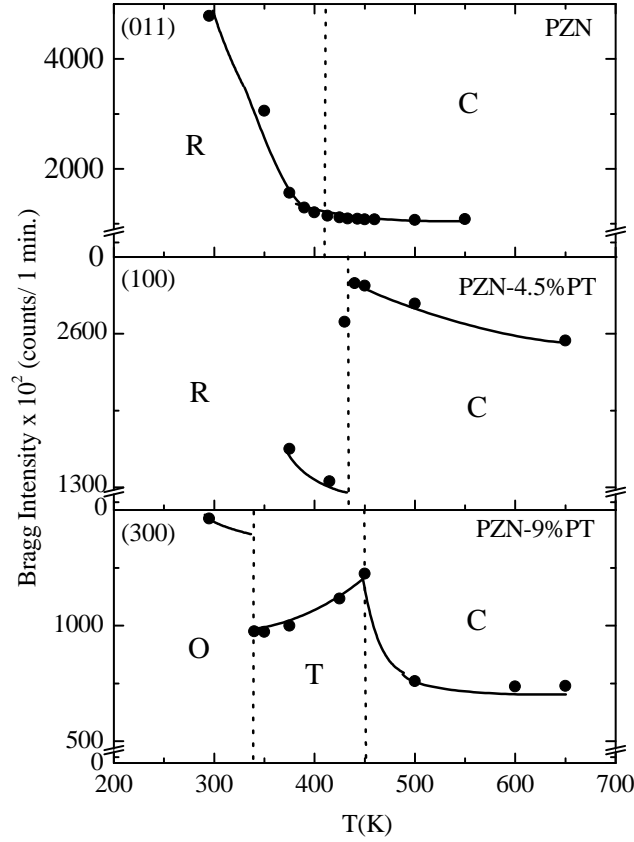


FIGURE 2. Temperature dependence of Bragg intensities for PZN at (011), PZN-4.5%PT at (100), and PZN-9%PT at (300) along the [111] directions, showing the phase transitions. Solid lines are drawn through the data points as guides to the eye. Dashed lines mark the phase transitions.

field important for ferroelectric phase transition. It is this strain field that induces the real phase transition characterized by the long range structural order. The transition temperatures observed in the present work are in good agreement with those previously reported [19].

The observed diffuse scattering has been explained by the presence of polar nanoregions, resulting from the short-range correlated atomic shifts [10, 16]. The reciprocal lattice points near which diffuse scattering is observed provide information about the internal structure of the regions. The width of the diffuse scattering gives us idea about the spatial extension of these regions in different directions, i.e. their orientation. In order to obtain information about the size of the polar regions, we have fitted the spectra with a combination of a Gaussian (Bragg) and a Lorentzian (diffuse), convoluted with the experimental resolution function. A Lorentzian lineshape is predicted by the Ornstein-Zernike model [20]:

$$I \simeq \frac{1}{q^2 + \xi^{-2}} \quad (1)$$

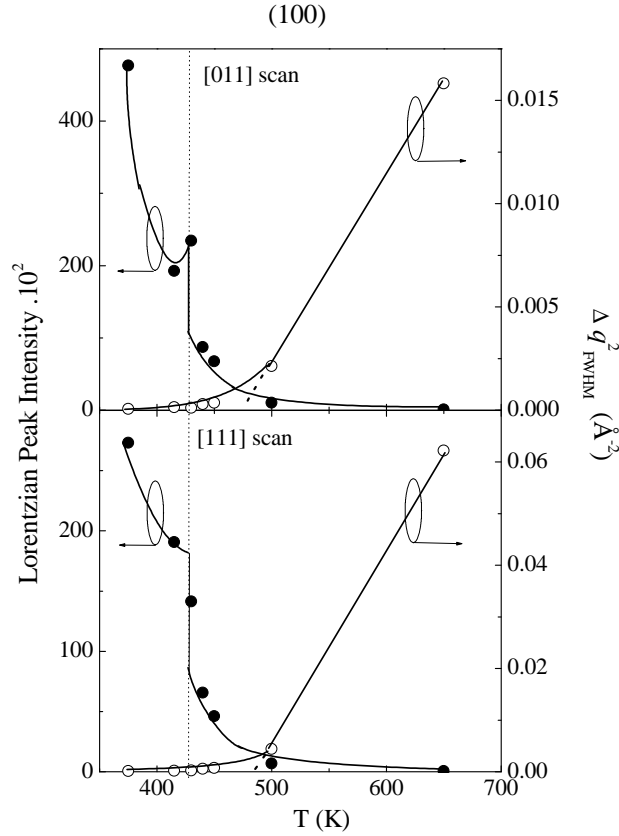


FIGURE 3. Lorentzian Peak Intensity and square of the FWHM, Δq_{FWHM}^2 vs. temperature for PZN-4.5%PT at the (100) point along the scan along the [011] and [111] directions.

where $q \equiv h$ is the momentum transfer relative to the $\mathbf{Q} = (011)$ Bragg reflection and ξ is the correlation length. This model assumes a correlation function of the form:

$$\frac{e^{-\frac{r}{\xi}}}{r}. \quad (2)$$

Therefore the diffuse scattering width at half maximum, Δq_{FWHM} , provides an estimate of ξ or, equivalently, of the size of the polar nanoregions:

$$\xi = \frac{2}{\Delta q_{FWHM}}, \quad (3)$$

where Δq in Eq.(3) is in units of $\frac{2\pi}{a}$. The diffuse scattering intensity is generally proportional to average polarization squared $\langle P_{local}^2 \rangle$. An increase of the diffuse scattering intensity with decreasing temperature reflects the growth of the polar clusters or growing correlation of atomic displacements. Below a certain temperature, T_f , the size of the polar regions stabilizes, as indicated by a constant width of the diffuse scattering

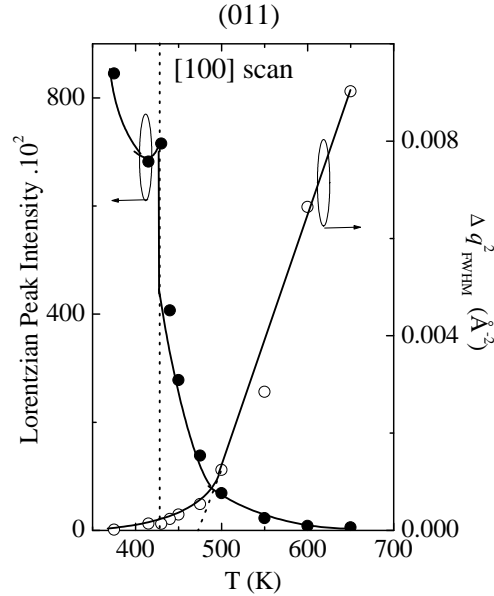


FIGURE 4. Lorentzian Peak Intensity and square of the FWHM, Δq_{FWHM}^2 vs. temperature for PZN-4.5%PT at the (011) point along the [100] direction.

peak. In the PZN system, the strongest diffuse scattering is primarily associated with the short-range correlated displacements of the Pb atoms along [111] direction [12]. For PZN-4.5%PT, the diffuse scattering becomes stronger in the transverse than in the [111] directions as shown on the left side of Fig. 3. This figure presents the temperature dependence of the diffuse scattering in PZN-4.5%PT at the (100) reflection in the transverse and [111] directions. In both directions, the diffuse scattering intensity increases continuously at first, and then goes through a cusp at the transition. The cusp is less pronounced in the [111] than in the transverse direction, looking more like a discontinuity in slope. It is important to note that intensity in the transverse direction is stronger than that in the [111] direction. Therefore, upon substitution of Ti^{4+} for $(Zn_{1/3}^{2+}/Nb_{2/3}^{5+})^{4+}$ at the B-site position, a change in symmetry of the primary distortion occurs. We have also found [12] that at high temperature the correlation length squared (ξ^2) follows a Curie-Weiss law. This suggests that the polar nanoregions are highly dynamics, since Δq_{FWHM}^2 is inversely proportional to ξ^2 , which is itself proportional to the dielectric constant, ϵ :

$$\Delta q_{FWHM}^2 \sim \frac{1}{\epsilon} = \frac{T - T_c}{C} \quad (4)$$

where C is the Curie constant. Therefore, the deviation from the linear dependence confirms the appearance of long-lived polar fluctuations at $T^* = T_c + \delta T$ in the crystal, accompanied by local strain fields. With PT addition, δT increases from ~ 40 K (in PZN[12]) to ~ 70 K (in PZN-4.5%PT as shown on the right side of Fig. 3 and 4). It means the process of slowing down in PZN- x PT begins at higher temperature than in

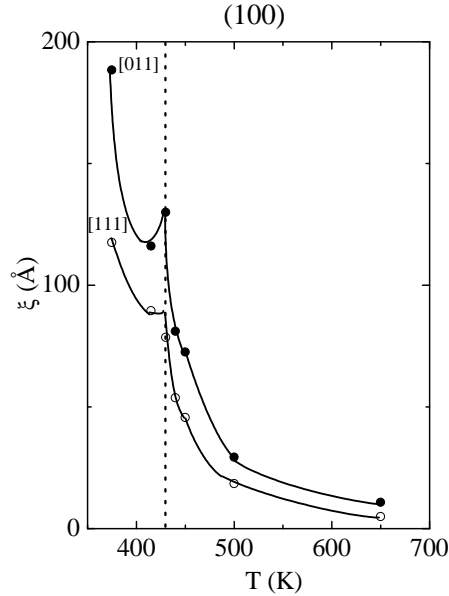


FIGURE 5. Temperature dependence of the correlation length, ξ for PZN-4.5%PT at the (100) reciprocal lattice point along the [011] and [111] directions.

pure PZN. This fact can be ascribed to the enhanced correlations between polar clusters induced by the presence of PT. This is in agreement to the similar results on PZN and PZN-10%PT single crystals deduced from the Vogel-Fulcher relation by Seo *et al* [21]. They have shown that the static freezing temperature (T_f) in PZN ($T_f=240$ K) is lower than that in PZN-10%PT ($T_f=297$ K).

In Fig. 5, we present the temperature dependence of the correlation length for PZN-4.5%PT at the (100) reflection along the transverse and diagonal directions. At the temperature T^* , the size of these regions is finite, about 29 Å (~ 7 unit cells) and 18 Å (~ 4 unit cells) along the transverse and diagonal directions, respectively. As the temperature decreases, the correlation lengths increase continuously at first, and then go through a cusp at the transition. In phase transition phenomena, cusps often indicate the occurrence of a condensation (see e.g. the liquid-gas transition, with a possible supercooled vapor phase).

In this study we have shown that the polar regions in PZN are preferentially more extended in the [111] than in the transverse direction, which is consistent with the [111] displacement of the Pb atom. However, with the addition of PT, the preferred orientation of the regions switches to the transverse direction. Nonetheless, the present diffuse neutron scattering results suggest that, upon going from PZN to PZN- x PT, the local polarizations (i.e. in the polar nanoregions) still retain an internal rhombohedral symmetry. This is suggested by the fact that, so far, the diffuse scattering has been observed at the same reciprocal points (100), (011), and, (300) in PZN and PZN- x PT. If this observation is confirmed, this would mean that, with increasing PT, the

polarization direction does not rotate, but that the regions preferentially grow in a different direction. Expressed differently, with the addition of PT, the polarization is still pointing in the [111] direction but the polar regions become longer in the transverse than in the [111] direction. This should have a positive effect on the ease of reorientation of this polarization, making it easier in PZN-*x*PT than in pure PZN. Before this point can be settled, additional measurements need to be performed in a different scattering zone.

ACKNOWLEDGMENTS

This research has been supported by DOE under Contract No. DE-FG02-00ER45842 for the experimental part and by ONR under Grant No. N00014-99-1-0738 for the crystal growth. We acknowledge the support of NIST Center for Neutron Research and Oak Ridge National Laboratory, in providing the neutron facilities used in this work and also thank R.K. Pattnaik, and O. Svitelskiy for their helpful suggestions.

REFERENCES

1. S.-E. Park and T.R. Shrout, *J. Appl. Phys.* **82**, 1804 (1997).
2. J. Kuwata, K. Uchino, and S. Nomura, *Jpn. J. Appl. Phys.* **21**, 1298 (1982).
3. S-F. Liu, S.-E. Park, T.R. Shrout, and L.E. Cross, *J. Appl. Phys.* **85**, 2810 (1999).
4. B. Noheda, Z. Zhong, D.E. Cox, G. Shirane, S.-E. Park, and P. Rehring, *Phys. Rev. B.* (inpress). cond-mat/0201182.
5. D.E. Cox, B. Noheda, G. Shirane, Y. Uesu, K. Fujishiro, and Y. Yamada, *Appl. Phys. Lett* **79**, 400 (2001).
6. D. La-Orautapong, B. Noheda, Z.-G. Ye, P.M. Gehring, J. Toulouse, D.E. Cox, and G. Shirane, *Phys. Rev. B.* **65**, 144101 (2002).
7. H. Fu and R. Cohen, *Nature* **403**, 281 (2000).
8. D. Vanderbilt and M. H. Cohen, *Phys. Rev. B.* **63**, 094108 (2001).
9. G. Burns and F.H. Dacol, *Phys. Rev. B.* **28**, 853 (1983).
10. N. de Mathan, E. Husson, G. Calvarin, J. R. Gavarri, A.W. Hewat, and A. Morell, *J. Phys.: Condens. Matter* **3**, 8159 (1991).
11. H. You and Q. M. Zhang, *Phys. Rev. Lett.* **79**, 3950 (1997).
12. D. La-Orautapong, J. Toulouse, J.L. Robertson, and Z.-G. Ye, *Phys. Rev. B.* **64**, 212101 (2001).
13. L. Zhang, M. Dong and Z.-G. Ye, *Mater. Sci. Eng. B.* **78**, 96 (2000).
14. W. Chen and Z.-G. Ye, *J. Mater. Sci.* **36**, 4393 (2001).
15. S.B. Vakhrushev, A.A. Naberezhnov, N.M. Okuneva, and B.N. Savenko, *Phys. Solid State* **37**, 1993 (1995).
16. G. Yong, J. Toulouse, R. Erwin, S. Shapiro, and B. Hennion, *Phys. Rev. B* **62**, 14736 (2000).
17. K. Hirota, Z.-G. Ye, S. Wakimoto, P.M. Gehring, and G. Shirane, *Phys. Rev. B.* **65**, 104105 (2002).
18. M.A. Krivoglaz, *Theory of X-Ray and Thermal-Neutron Scattering by Real Crystals*, Plenum Press, New York, 1969.
19. J. Kuwata, K. Uchino, and S. Nomura, *Ferroelectrics* **37**, 579 (1981).
20. H.E. Stanley, *Introduction to Phase Transitions and Critical Phenomena*, Oxford University Press, New York, 1971.
21. S. -A. Seo, K. H. Noh, and S.-II Kwun, *J. Korean Phys. Soc.* **35**, 496 (1999).